Fault Tolerant Control of a PEM Fuel Cell using qLPV Virtual Actuators

Damiano Rotondo * **Vicenç Puig** *,** **Fatiha Nejjari** *

* *Automatic Control Department, Universitat Politècnica de Catalunya (UPC), Rambla de Sant Nebridi, 11, 08222 Terrassa, Spain.*
** *Institute of Robotics and Industrial Informatics, Edifici U, Pau Gargallo, 5, 08028-Barcelona, Spain*

Abstract:
This paper proposes a fault tolerant control (FTC) strategy based on the use of quasi-linear parameter varying (qLPV) virtual actuators approach for proton exchange membrane (PEM) fuel cells. The overall solution relies on adding a virtual actuator in the control loop to hide the fault from the controller point of view, allowing it to see the same plant as before the fault, in this way keeping the stability and some desired performances. The proposed methodology is based on the use of a reference model, where the resulting nonlinear error model is brought to a qLPV form that is used for control design by means of linear matrix inequalities (LMI)-based techniques. The resulting closed-loop error system is stable with poles placed in some desired region of the complex plane. Simulation results are used to show the effectiveness of the proposed approach.

Keywords: LPV model, Virtual actuator, Reference model based control, Gain-scheduling, PEM Fuel Cell, LMIs.

1. INTRODUCTION

Fuel cells supply electricity to a load by converting chemical energy into a silent, lower-emission, high-efficiency power source. Many control loops are included in the system to take care of fuel/air feeding, humidity, pressure and temperature (lower control level), as well as integrating the electrical conditioning, storage and reformer (upper control level).

Fuel cells are very complex systems, which may be affected by component faults, that can cause serious damage, leading to their stop (Feroldi, 2012). Hence, it is important to include some fault tolerant mechanisms into the control system, such that the fuel cell can still operate under fault occurrence (Puig et al., 2007). Fault tolerant control (FTC) techniques allow to maintain stability and acceptable performances in the event of such faults (Blanke et al., 2006; Noura et al., 2009).

Among the paradigms proposed in the recent literature, the *fault-hiding* one has attracted some attention as an active strategy to obtain fault tolerance (Steffen, 2005). The goal of this paradigm is to reconfigure the faulty plant instead of the controller/observer. Thus, a reconfiguration block is inserted between the faulty plant and the nominal controller/observer under fault occurrence, such that the nominal controller can be kept in the control loop without the need of retuning it. When the reconfiguration block aims at tolerating actuator faults, it is named *virtual actuator*. Initially proposed in a state space form for LTI systems (Lunze and Steffen, 2006), this paradigm has been successfully extended to other system structures (Rotondo et al., 2014; Dziekan et al., 2011; Richter et al., 2011; Blesa et al., 2014).

In order to deal with the nonlinear dynamics of fuel cells, described in detail in Pukrushpan et al. (2004), linear parameter varying (LPV) design techniques have been investigated, not only for control (Bianchi et al., 2014), but also for model-based fault diagnosis (de Lira et al., 2011).

This paper proposes an FTC strategy for proton exchange membrane (PEM) fuel cells based on a combination of the virtual actuator and LPV paradigms. The proposed solution relies on a reconfigured reference model that provides the reference signals to be tracked. The resulting nonlinear error model is transformed into a quasi-LPV one using a gridding approach. Then, using linear matrix inequalities (LMIs)-based design techniques, a controller can be designed for the quasi-LPV error model in order to guarantee stability of the resulting closed-loop system, while attaining some desired properties, e.g. pole clustering in a desired region of the complex plane. The effectiveness of the proposed approach is demonstrated using simulation results.

The structure of the paper is the following. The PEM Fuel Cell description and nonlinear model, as well as its quasi-LPV representation, are presented in Section 2. It is also shown how, using a reference model, an error model that will be used for designing an error-feedback controller can be obtained. Section 3 describes the error-feedback controller design using LMI-based techniques. Section 4 presents the proposed FTC strategy based on virtual actuators. The application to a PEM Fuel Cell case study and the simulation results are presented in Section 5. Finally, Section 6 outlines the main conclusions.

⋆ This work has been funded by the Spanish Ministry of Science and Technology through the project through the projects ECOCIS (Ref. DPI2013-48243-C2-1-R) and HARCRICS (Ref. DPI2014-58104-R), by AGAUR through the contract FI-DGR 2014 (ref. 2014FI B1 00172) and by the DGR of Generalitat de Catalunya (SAC group Ref. 2014/SGR/374).
e-mail: damiano(dot)rotondo(at)yahoo(dot)it

2. PEM FUEL CELL LPV MODELLING

The basic physical structure of a fuel cell consists of an electrolyte layer in contact with a porous anode and cathode electrode plates. There are different kinds of electrolyte layers. Here a PEM (Polymer Electrolyte Membrane or Proton Exchange Membrane) fuel cell is used. The PEM has a special property: it conducts protons but is impermeable to gas (the electrons are blocked through the membrane). Auxiliary devices are required to ensure the proper operation of the fuel cell stack: an air compressor, a hydrogen tank, a supply manifold and a return manifold.

2.1 Non-linear and quasi-LPV modeling of PEM Fuel Cell

The control model used in this work is derived from the one presented in Pukrushpan et al. (2004), and has three state variables: the pressure in the supply manifold p_{sm} (Pa), the pressure in the return manifold p_{rm} (Pa) and the mass of oxygen in the cathode m_{O_2} (kg). The compressor mass flow W_{cp} (kg/s) and the return manifold outlet orifice constant $k_{rm,out}$ (ms) are considered control variables while the current in the stack I_{st} (A) represents a third input variable, that can be considered as a disturbance input to be included in the reference model, in order to generate an appropriate feedforward action, and make the feedback loop insensitive to its variation:

$$\begin{aligned}\dot{p}_{sm} = {} & \frac{\gamma R_a}{V_{sm}} W_{cp} \left[T_{atm} + \frac{T_{atm}}{\eta_{cp}} \left[\left(\frac{p_{sm}}{p_{atm}} \right)^{\frac{\gamma-1}{\gamma}} - 1 \right] \right] \\ & - \frac{\gamma R_a}{V_{sm}} k_{sm,out} \left(p_{sm} - \frac{m_{O_2} R_{O_2} T_{st}}{V_{ca}} \right) T_{sm}\end{aligned} \tag{1}$$

$$\begin{aligned}\dot{p}_{rm} = {} & \frac{R_a T_{rm}}{V_{rm}} k_{ca,out} \left(\frac{m_{O_2} R_{O_2} T_{st}}{V_{ca}} - p_{rm} \right) \\ & - \frac{R_a T_{rm}}{V_{rm}} k_{rm,out} \left(p_{rm} - p_{atm} \right)\end{aligned} \tag{2}$$

$$\begin{aligned}\dot{m}_{O_2} = {} & k_{sm,out} p_{sm} - \frac{m_{O_2} R_{O_2} T_{st}}{V_{ca}} (k_{sm,out} + k_{ca,out}) \\ & + k_{ca,out} p_{rm} - M_{O_2} \frac{n I_{st}}{4F}\end{aligned} \tag{3}$$

The nonlinear model (1)-(3) can be expressed in a quasi-linear parameter varying [1] (qLPV) representation using the nonlinear embedding in the parameters approach (Kwiatkowski et al., 2006), as follows:

$$\dot{x} = Ax(t) + B(\theta(t))u(t) + cw(t) \tag{4}$$

with $x(t) = [p_{sm}(t), p_{rm}(t), m_{O_2}(t)]^T$, $u(t) = [W_{cp}(t), k_{rm,out}(t)]^T$, $w(t) = I_{st}(t)$, and state-space matrices as follows:

$$A = \begin{pmatrix} a_{11} & 0 & a_{13} \\ 0 & a_{22} & a_{23} \\ a_{31} & a_{32} & a_{33} \end{pmatrix} \quad B(\theta) = \begin{pmatrix} \theta_1 & 0 \\ 0 & \theta_2 \\ 0 & 0 \end{pmatrix} \quad c = -\frac{M_{O_2} n}{4F} \tag{5}$$

$$a_{11} = -\frac{\gamma R_a}{V_{sm}} k_{sm,out} T_{sm} \quad a_{13} = -a_{11} \frac{R_{O_2} T_{st}}{V_{ca}}$$

$$a_{22} = -\frac{R_a T_{rm}}{V_{rm}} k_{ca,out} \quad a_{23} = -a_{22} \frac{R_{O_2} T_{st}}{V_{ca}}$$

$$a_{31} = k_{sm,out} \quad a_{32} = k_{ca,out} \quad a_{33} = -(a_{31} + a_{32}) \frac{R_{O_2} T_{st}}{V_{ca}}$$

[1] The term *quasi* refers to the fact that the varying parameters are functions of some endogenous signals, i.e. state variables.

$$\theta_1(t) = \frac{\gamma R_a}{V_{sm}} \left[T_{atm} + \frac{T_{atm}}{\eta_{cp}} \left[\left(\frac{p_{sm}(t)}{p_{atm}} \right)^{\frac{\gamma-1}{\gamma}} - 1 \right] \right]$$

$$\theta_2(t) = -\frac{R_a T_{rm}}{V_{rm}} k_{rm,out} \left(p_{rm}(t) - p_{atm} \right)$$

It is assumed that the vector $\theta(t) = [\theta_1(t), \theta_2(t)]^T$ belongs to a bounded set Θ, known a priori.

2.2 Reference and error quasi-LPV models

The reference model provides the state trajectory to be tracked by the PEM fuel cell, starting from the reference inputs $W_{cp}^{ref}(t)$ and $k_{rm,out}^{ref}(t)$. The values of the reference inputs to be fed to the reference model (feedforward actions) are obtained from steady-state considerations about the fuel cell system, so as to keep the supply manifold pressure and the oxygen stoichiometry, defined as follows:

$$\lambda_{O_2}(t) = \frac{k_{sm,out} \left(p_{sm}(t) - \frac{m_{O_2}(t) R_{O_2} T_{st}}{V_{ca}} \right)}{M_{O_2} \frac{n I_{st}(t)}{4F}} \tag{6}$$

at some desired values p_{sm}^{∞} and $\lambda_{O_2}^{ref}$.

In this work, the reference model is chosen as follows:

$$\dot{x}_{ref}(t) = Ax_{ref}(t) + B(\theta(t))u_{ref}(t) + cw(t) \tag{7}$$

with $x_{ref}(t) = \left[p_{sm}^{ref}(t), p_{rm}^{ref}(t), m_{O_2}^{ref}(t) \right]^T$ and $u_{ref}(t) = [W_{cp}^{ref}(t), k_{rm,out}^{ref}(t)]^T$.

Then, by subtracting the reference model equations (7) and the corresponding system equations (4), and by defining the tracking error vector $e(t) \triangleq x_{ref}(t) - x(t)$ and the new input vector $\Delta u(t) \triangleq u_{ref}(t) - u(t)$, the following qLPV error system is obtained:

$$\dot{e}(t) = Ae(t) + B(\theta(t))\Delta u(t) \tag{8}$$

that can be discretized using an Euler approach with sampling time T_s, leading to the following discrete-time model:

$$e(k+1) = A_d e(k) + B_d(\theta(k))\Delta u(k) \tag{9}$$

with $A_d = I + AT_s$ and $B_d(\theta(k)) = B(\theta(k))T_s$.

3. CONTROLLER DESIGN USING LMI-BASED TECHNIQUES

The following error-feedback controller is proposed for the discrete-time error system (9):

$$\Delta u_c(k) = K(\theta(k))e(k) \tag{10}$$

The controller (10) is designed using an LMI-based approach, where the desired specifications are guaranteed using the results from the quadratic Lyapunov framework (Tanaka and Wang, 2001). Despite the introduction of conservativeness with respect to other existing approaches, the quadratic approach has undeniable advantages in terms of computational complexity.

For the synthesis of the controller, N operating points are considered for the error system (9), such that for each of them, a local LTI model is obtained [2]:

[2] This approach is usually referred to as *gridding approach*. Even though the stability and desired performance are strictly guaranteed only at the design points, when the gridding is sufficiently dense, it is reasonable to assume that stability and performance will still hold at operating points different from the design ones.

$$e(k+1) = A_d e(k) + B_i \Delta u(k) \quad i = 1,\ldots,N \tag{11}$$

such that the following holds:

$$B_d(\theta(k)) = \sum_{i=1}^{N} \mu_i(\theta(k)) B_i \tag{12}$$

with:

$$\sum_{i=1}^{N} \mu_i(\theta) = 1, \quad \mu_i(\theta) \geq 0 \qquad \begin{matrix} \forall i = 1,\ldots,N \\ \forall \theta \in \Theta \end{matrix} \tag{13}$$

Then, the qLPV error system (9) with input matrix as in (12), with the error-feedback controller (10) with gain chosen as:

$$K(\theta(k)) = \sum_{i=1}^{N} \alpha_i(\theta(k)) K_i \tag{14}$$

is quadratically stable if there exist $X > 0$ and $K_i, i = 1,\ldots,N$ such that:

$$\begin{pmatrix} -X & (A_d + B_i K_i) X \\ X (A_d + B_i K_i)^T & -X \end{pmatrix} < 0 \quad \forall i = 1,\ldots,N \tag{15}$$

On the other hand, pole clustering is based on the results obtained by Chilali and Gahinet (1996), where subsets $\mathscr{D}$ of the complex plane, referred to as *LMI regions*, are defined as:

$$\mathscr{D} = \{z \in \mathbb{C} : f_{\mathscr{D}}(z) < 0\} \tag{16}$$

where $f_{\mathscr{D}}$ is the *characteristic function*, defined as:

$$f_{\mathscr{D}}(z) = \alpha + z\beta + \bar{z}\beta^T = [\alpha_{hl} + \beta_{hl} z + \beta_{lh} \bar{z}]_{h,l \in [1,m]} \tag{17}$$

with $\alpha = \alpha^T \in \mathbb{R}^{m \times m}$ and $\beta \in \mathbb{R}^{m \times m}$.

Hence, the qLPV error system (9) with an input matrix as in (12), with the error-feedback controller (10) with a gain chosen as in (14), has poles in $\mathscr{D}$ if there exist $X_{\mathscr{D}} > 0$ and K_i, $i = 1,\ldots,N$, such that:

$$\left[\alpha_{hl} X_{\mathscr{D}} + \beta_{hl} (A_d + B_i K_i) X_{\mathscr{D}} + \beta_{lh} X_{\mathscr{D}} (A_d + B_i K_i)^T\right]_{h,l \in [1,m]} < 0 \tag{18}$$

for $i = 1,\ldots,N$.

Conditions (15) and (18) are bilinear matrix inequalities (BMIs) that can be brought to linear matrix inequalities (LMIs) form by using a single Lyapunov matrix $X = X_{\mathscr{D}} > 0$ and through the change of variables $\Gamma_i \triangleq K_i X$:

$$\begin{pmatrix} -X & A_d X + B_i \Gamma_i \\ (A_d X + B_i \Gamma_i)^T & -X \end{pmatrix} < 0 \tag{19}$$

$$\left[\alpha_{hl} X + \beta_{hl} (A_d X + B_i \Gamma_i) + \beta_{lh} (A_d X + B_i \Gamma_i)^T\right]_{h,l \in [1,m]} < 0 \tag{20}$$

that can be solved using available software, e.g. the YALMIP toolbox (Löfberg, 2004) with SeDuMi solver (Sturm, 1999).

4. FAULT TOLERANT CONTROL USING LPV VIRTUAL ACTUATORS

4.1 Including faults in the model

Two types of actuator faults are considered: changes in the effectiveness of the faulty actuators, and stuck faults, where the inputs delivered by the faulty actuators are blocked to constant values. In the first case, the faulty model is as follows:

$$\dot{x}(t) = Ax(t) + B_f(\theta(t), \phi(t)) u(t) + cw(t) \tag{21}$$

with:

$$B_f(\theta(t), \phi(t)) = B(\theta(t)) diag(\phi_1(t), \ldots, \phi_{n_u}(t)) \tag{22}$$

where $\phi_j(t) \in]0,1]$ represents the effectiveness of the jth actuator, such that the value $\phi_j = 1$ represents the healthy situation.

In the second case, the faulty model is:

$$\dot{x}(t) = Ax(t) + B^*(\theta(t)) u(t) + [B(\theta(t)) - B^*(\theta(t))] \bar{u}(t) + cw(t) \tag{23}$$

where $\bar{u}(t)$ is the vector containing the values of the stuck control inputs and $B^*(\theta(t))$ is the matrix obtained from $B(\theta(t))$ by replacing the columns corresponding to the stuck actuators with zero vectors.

Then, in the case of multiplicative faults, the reference model is changed as follows:

$$\dot{x}_{ref}(t) = Ax_{ref}(t) + B_f\left(\theta(t), \hat{\phi}(t)\right) u_{ref}(t) + cw(t) \tag{24}$$

where $\hat{\phi}(t)$ is an estimation of the multiplicative actuator faults, while in the case of stuck faults, it becomes:

$$\begin{aligned} \dot{x}_{ref}(t) = {} & Ax_{ref}(t) + B^*(\theta(t)) u_{ref}(t) \\ & + [B(\theta(t)) - B^*(\theta(t))] \hat{\bar{u}}(t) + cw(t) \end{aligned} \tag{25}$$

where $\hat{\bar{u}}(t)$ is an estimation of the stuck actuator faults.

Then, under the assumption that $\hat{\phi}(t) \cong \phi(t)$ and $\hat{\bar{u}}(t) \cong \bar{u}(t)$ (the case where such an assumption does not hold, i.e. when there is uncertainty in the fault estimation, will be addressed by future research), the error model takes the form:

$$\dot{e}(t) = Ae(t) + B_f\left(\theta(t), \hat{\phi}(t)\right) \Delta u(t) \tag{26}$$

or:

$$\dot{e}(t) = Ae(t) + B^*(\theta(t)) \Delta u(t) \tag{27}$$

for multiplicative or stuck faults, respectively.

Then, using an Euler approach with sampling time T_s, discrete-time versions of (26) and (27) can be obtained as:

$$e(k+1) = A_d e(k) + B_{fd}\left(\theta(k), \hat{\phi}(k)\right) \Delta u(k) \tag{28}$$

and:

$$e(k+1) = A_d e(k) + B_d^*(\theta(k)) \Delta u(k) \tag{29}$$

respectively, with:

$$B_{fd}\left(\theta(k), \hat{\phi}(k)\right) = B_f\left(\theta(k), \hat{\phi}(k)\right) T_s \tag{30}$$

and:

$$B_d^*(\theta(k)) = B^*(\theta(k)) T_s \tag{31}$$

4.2 Virtual actuator design

The main idea of the virtual actuator FTC method, first introduced in Lunze and Steffen (2006), is to reconfigure the faulty plant such that the nominal controller could still be used without need of retuning it. The plant with the faulty actuators is modified adding the virtual actuator block that masks the fault and allows the controller to see the same plant as before the fault.

In the case of multiplicative faults, the virtual actuator is static since the following condition is satisfied:

$$rank(B_{fd}(\theta(k), \hat{\phi}(k))) = rank\begin{pmatrix} B_d(\theta(k)) & B_{fd}(\theta(k), \hat{\phi}(k)) \end{pmatrix} \tag{32}$$

and it can be expressed as:

$$\Delta u(k) = N_v(\theta(k), \hat{\phi}(k)) \Delta u_c(k) \tag{33}$$

where $\Delta u_c(k)$ is the controller output provided by (10) and:

$$N_v(\theta(k), \hat{\phi}(k)) = B_{fd}^{\dagger}(\theta(k), \hat{\phi}(k)) B_d(\theta(k)) \tag{34}$$

where the symbol † denotes the Moore-Penrose pseudoinverse. In this case, the fault-hiding property is achieved thanks to the multiplicative faults effects compensation brought by (34).

On the other hand, in the case of stuck faults, the fault tolerance is achieved using the reconfiguration structure expressed by:

$$\Delta u(k) = N_v(\theta(k), \hat{\phi}(k))(\Delta u_c(k) - M_v(\theta(k))x_v(k)) \tag{35}$$

where the virtual actuator state $x_v(k)$ is obtained through:

$$\begin{aligned} x_v(k+1) = &[A_d(\theta(k)) + B_d^*(\theta(k))M_v(\theta(k))]x_v(k) \\ &+ [B_d(\theta(k)) - B_d^*(\theta(k))]\Delta u_c(k) \end{aligned} \tag{36}$$

Moreover, in order to achieve the fault-hiding property, the signal entering into the controller is slightly modified, such that the outputs of the controller become as follows:

$$\Delta u_c(k) = K(\theta(k))(e(k) + x_v(k)) \tag{37}$$

When the stuck fault occurs, the virtual actuator reconstructs the vector $\Delta u(k)$ from the outputs of the nominal controller $\Delta u_c(k)$, taking into account the fault occurrence. The faulty plant and the virtual actuator are called the *reconfigured plant*, which is connected to the nominal controller. If the reconfigured plant behaves like the nominal plant, the loop consisting of the reconfigured plant and the controller behaves like the nominal closed-loop system.

4.3 Reconfiguration Analysis

In the following, it is shown that thanks to the introduction of the virtual actuator block, the augmented system can be brought to a block-triangular form.

Theorem 1. Consider the augmented system made up by the faulty error system (29), the reconfiguration structure (35), the virtual actuator state equation (36) and the control law (37) [3]:

$$\begin{pmatrix} e(k+1) \\ x_v(k+1) \end{pmatrix} = \begin{pmatrix} A_d + B_d^* K & B_d^*(K - M_v) \\ (B_d - B_d^*)K & A_d + B_d^* M_v + (B_d - B_d^*)K \end{pmatrix} \begin{pmatrix} e(k) \\ x_v(k) \end{pmatrix} \tag{38}$$

Then, there exists a similarity transformation such that the state matrix of the augmented system in the new state variables is block-triangular, as follows:

$$A_{aug} = \begin{pmatrix} A_d + B_d K & 0 \\ (B_d - B_d^*)K & A_d + B_d^* M_v \end{pmatrix} \tag{39}$$

Proof: The proof is straightforward, and comes from introducing the new state variable $x_1(k) \triangleq e(k) + x_v(k)$ and considering the state $(\, x_1(k) \;\; x_v(k) \,)^T$. ■

Looking at (39), it can be seen that the state $x_1(k)$ is affected by K through the matrix $A_d + B_d K$, while the state $x_v(k)$ is affected by M_v through the matrix $A_d + B_d^* M_v$. Hence, the controller and the virtual actuator can be designed independently.

The design conditions presented in Section 3 can be applied to the case of virtual actuator design by making the changes $B_d \to B_d^*$ and $K \to M_v$.

5. RESULTS

The values used in this work have been taken from Aitouche et al. (2011), and are listed in Table 1.

[3] The dependence of the matrices A_d, B_d, B_d^*, K and M_v on the varying parameter vector $\theta(k)$ has been omitted for lack of space.

Table 1. List of parameters and values

Variable	Description	Value and Unit
η_{cp}	Compressor efficiency	0.8
γ	Specific heat capacity of gas	1.4
R_a	Air gas constant	$286.9 J/(kgK)$
R_{O_2}	Oxygen gas constant	$259.8 J/(kgK)$
V_{sm}	Supply manifold volume	$0.02 m^3$
V_{ca}	Cathode volume	$0.01 m^3$
V_{rm}	Return manifold volume	$0.005 m^3$
T_{atm}	Air temperature	$298.15 K$
T_{st}	Temperature in the stack	$350 K$
T_{sm}	Supply manifold temperature	$300 K$
T_{rm}	Return manifold temperature	$300 K$
p_{atm}	Air pressure	$101325 Pa$
$k_{sm,out}$	Supply manifold outlet flow constant	$0.3629 \cdot 10^{-5} kg/sPa$
$k_{ca,out}$	Cathode outlet flow constant	$0.2177 \cdot 10^{-5} kg/sPa$
M_{O_2}	Oxygen molar mass	$32 \cdot 10^{-3} kg/mol$
n	Cells in the FCS	381
F	Faraday constant	$96485 C/mol$

The nominal controller has been designed to assure stability and pole clustering in a circle of radius 0.4 and center $(0.599, 0)$. Moreover, since it is assumed that only p_{sm} and p_{rm} are measured, a state observer has been added to the control loop to obtain an estimation of m_{O2}.

The results shown in this paper refer to simulations that last $200 s$, where the current in the stack I_{st} and the desired oxygen stoichiometry $\lambda_{O_2}^{ref}(t)$ are varying in time as follows:

$$\left(I_{st}(t), \lambda_{O_2}^{ref}(t)\right) = \begin{cases} (150, 2) & t \leq 40s \\ (250, 2.5) & 40s < t \leq 80s \\ (200, 3) & 80s < t \leq 120s \\ (350, 2.5) & 120s < t \leq 160s \\ (300, 2) & 160s < t \leq 200s \end{cases} \tag{40}$$

and the desired supply manifold pressure is set to $p_{sm}^{\infty} = 1.5 Pa$.

In this work, three possible faults are considered.

5.1 Fault Scenario 1: loss of effectiveness of W_{cp}

In fault scenario 1, a loss of effectiveness $\phi_{cp} = 0.5$ appearing at time $t = 100 s$ has been considered.

By including this fault in the dynamic model of the PEM fuel cell, (1) becomes:

$$\begin{aligned} \dot{p}_{sm} = &\frac{\gamma R_a}{V_{sm}} \phi_{cp} W_{cp} \left[T_{atm} + \frac{T_{atm}}{\eta_{cp}} \left[\left(\frac{p_{sm}}{p_{atm}} \right)^{\frac{\gamma-1}{\gamma}} - 1 \right] \right] \\ &- \frac{\gamma R_a}{V_{sm}} k_{sm,out} \left(p_{sm} - \frac{m_{O_2} R_{O_2} T_{st}}{V_{ca}} \right) T_{sm} \end{aligned} \tag{41}$$

where ϕ_{cp} denotes the multiplicative fault of the air compressor flow.

Fig. 1 shows a comparison of the response of the oxygen excess ratio λ_{O_2} without the proposed FTC strategy and with the proposed FTC strategy. It can be seen that the loss of effectiveness of the actuator W_{cp} leads to an undesired offset between the desired $\lambda_{O_2}^{ref}$ and the real one. On the other hand, by calculating W_{cp} using the virtual actuator (blue line in Fig. 2), the fault is hidden and the real input after the loss of

effectiveness (red line in Fig. 2) equals the one obtained in nominal situation (black dots in Fig. 2).

5.2 Fault Scenario 2: loss of effectiveness of $k_{rm,out}$

In fault scenario 2, a loss of effectiveness $\phi_{rm,out} = 0.5$ appearing at time $t = 100\,s$ has been considered.

By including this fault, (2) changes to:

$$\begin{aligned}\dot{p}_{rm} = &\frac{R_a T_{rm}}{V_{rm}} k_{ca,out} \left(\frac{m_{O_2} R_{O_2} T_{st}}{V_{ca}} - p_{rm} \right) \\ &- \frac{R_a T_{rm}}{V_{rm}} \phi_{rm,out} k_{rm,out} \left(p_{rm} - p_{atm} \right)\end{aligned} \tag{42}$$

where $\phi_{rm,out}$ denotes the multiplicative fault of the return manifold outlet orifice.

Similarly to the case of fault scenario 1, an offset appears in the response of λ_{O_2} when no FTC strategy is applied (red line in Fig. 3). The reconfiguration of the control input brought by the virtual actuator (see Fig. 4) allows to eliminate the offset (blue line in Fig. 3).

5.3 Fault Scenario 3: stuck of $k_{rm,out}$

In fault scenario 3, the return manifold outlet is stuck starting from time $t = 100\,s$.

In this case, $k_{rm,out}$ is stuck to $\bar{k}_{rm,out}$, such that (2) becomes:

$$\begin{aligned}\dot{p}_{rm} = &\frac{R_a T_{rm}}{V_{rm}} k_{ca,out} \left(\frac{m_{O_2} R_{O_2} T_{st}}{V_{ca}} - p_{rm} \right) \\ &- \frac{R_a T_{rm}}{V_{rm}} \bar{k}_{rm,out} \left(p_{rm} - p_{atm} \right)\end{aligned} \tag{43}$$

As shown in Fig. 5, no effect is visible in the oxygen excess ratio response until a change in the reference $\lambda_{O_2}^{ref}$ occurs at time $t = 120\,s$. This fact is reasonable, because in the interval between the fault occurrence and the reference change, the return manifold outlet is stuck near the correct position that assures an error approximately zero. After the reference change, it can be seen that, although the stuck fault is not so critical as the multiplicative faults, the transient has become slower. The proposed virtual actuator strategy allows to improve the overall performance.

6. CONCLUSIONS

In this paper, an LPV virtual actuator FTC strategy for PEM fuel cells has been proposed. The overall solution relies on adapting the controller in order to keep the stability and some desired performances. The proposed methodology is based on the use of a reference model, where the resulting nonlinear error model is brought to a qLPV form for designing a controller using LMI-based techniques. Simulation results have shown that if no FTC strategy is applied, undesired offsets would appear in the case of multiplicative faults, and the transient would become slower in the case of the considered stuck fault. On the other hand, the proposed FTC strategy allows to improve the overall performance in both cases.

Future research will aim at increasing the robustness of the proposed strategy against exogenous disturbances and parametric uncertainty, with the goal of testing it using a real PEM fuel cell setup.

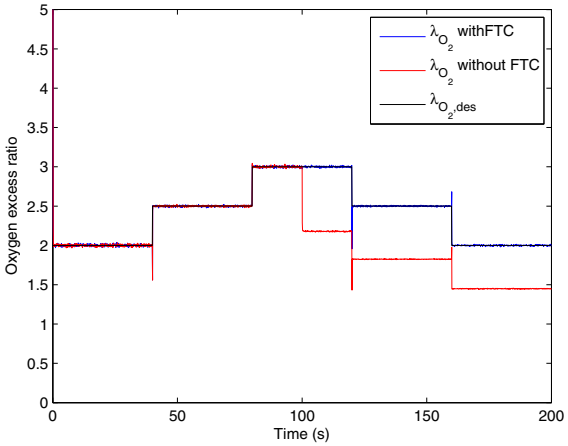

Fig. 1. Oxygen excess ratio with and without FTC in fault scenario 1 (Loss of effectiveness of W_{cp}).

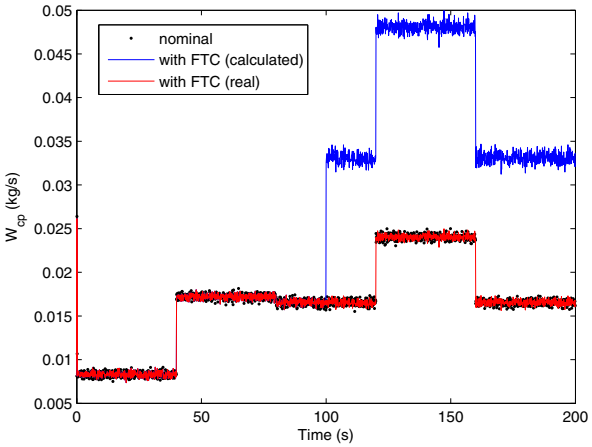

Fig. 2. Compressor mass flow with and without FTC in fault scenario 1 (Loss of effectiveness of W_{cp}).

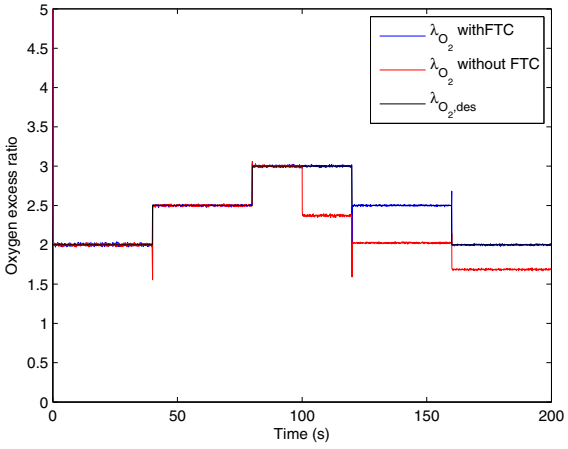

Fig. 3. Oxygen excess ratio with and without FTC in fault scenario 2 (Loss of effectiveness of $k_{rm,out}$).

REFERENCES

A. Aitouche, Q. Yang, and B. Ould Bouamama. Fault detection and isolation of PEM fuel cell system based on nonlinear analytical redundancy. *The European Physical Journal Applied*

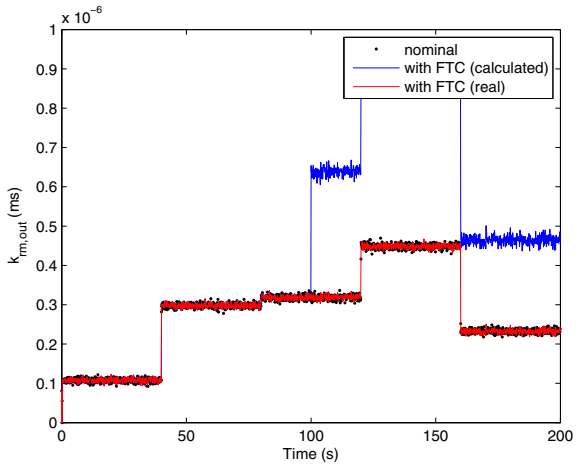

Fig. 4. Return manifold outlet orifice constant with and without FTC in fault scenario 2 (Loss of effectiveness of $k_{rm,out}$).

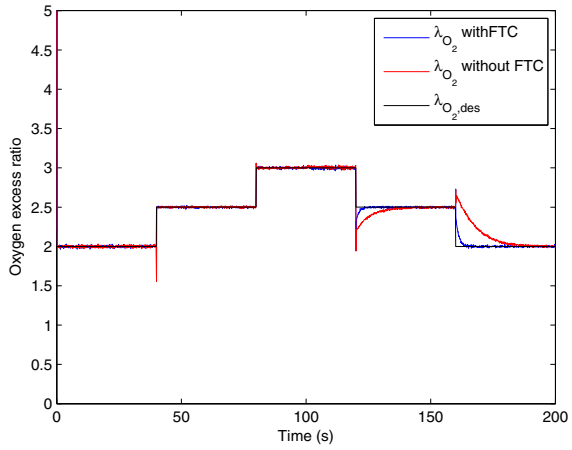

Fig. 5. Oxygen excess ratio with and without FTC in fault scenario 3 (Stuck of $k_{rm,out}$).

Physics, 54(2), 2011.

F. D. Bianchi, C. Kunusch, C. Ocampo-Martínez, and R. S. Sánchez-Peña. A gain-scheduled LPV control for oxygen stoichiometry regulation in PEM fuel cell systems. *IEEE Transactions on Control Systems Techonology*, (in preview), 2014.

M. Blanke, M. Kinnaert, J. Lunze, and M. Staroswiecki. *Diagnosis and Fault-Tolerant Control*. Springer-Verlag Berlin Heidelberg, 2006. ISBN 978-3-540-35652-3.

J. Blesa, D. Rotondo, V. Puig, and F. Nejjari. FDI and FTC of wind turbines using the interval observer approach and virtual actuators/sensors. *Control Engineering Practice*, 24: 138–155, 2014.

M. Chilali and P. Gahinet. H_∞ design with pole placement constraints: an LMI approach. *IEEE Transactions on Automatic Control*, 41(3):358–367, 1996.

S. de Lira, V. Puig, J. Quevedo, and A. Husar. LPV observer design for PEM fuel cell system: Application to fault detection. *Journal of Power Sources*, 196(9):4298 – 4305, 2011.

Ł. Dziekan, M. Witczak, and J. Korbicz. Active fault-tolerant control design for Takagi-Sugeno fuzzy systems. *Bulletin of the Polish Academy of Sciences*, 59(1):93–102, 2011.

D. Feroldi. Fault diagnosis and fault tolerant control of PEM fuel cell systems. In M. S. Basualdo, D. Feroldi, and R. Outbib, editors, *PEM fuel cells with bio-ethanol processor systems*, pages 185–206. Springer, 2012.

A. Kwiatkowski, M.-T. Boll, and H. Werner. Automated Generation and Assessment of Affine LPV Models. In *Proceedings of the 45th IEEE Conference on Decision and Control*, pages 6690–6695, 2006.

J. Löfberg. YALMIP: A toolbox for modeling and optimization in MATLAB. In *Proceedings of the CACSD Conference*, 2004.

J. Lunze and T. Steffen. Control reconfiguration after actuator failures using disturbance decoupling methods. *IEEE Transactions on Automatic Control*, 51(10):1590–1601, 2006.

H. Noura, D. Theilliol, J. C. Ponsart, and A. Chamseddine. *Fault-tolerant control systems: Design and practical applications*. Springer London, 2009.

V. Puig, A. Rosich, C. Ocampo-Martínez, and R. Sarrate. Fault-tolerant explicit mpc of pem fuel cells. In *Proceedings of the 46th IEEE Conference on Decision and Control*, pages 2657–2662, 2007.

J. T. Pukrushpan, H. Peng, and A. G. Stefanopoulou. Control-oriented modeling and analysis for automotive fuel cell systems. *ASME Journal of Dynamic Systems, Measurement and Control*, 126(1):14–25, 2004.

J. H. Richter, W. P. M. H. Heemels, N. van de Wouw, and J. Lunze. Reconfigurable control of piecewise affine systems with actuator and sensor faults: stability and tracking. *Automatica*, 47:678–691, 2011.

D. Rotondo, F. Nejjari, and V. Puig. A virtual actuator and sensor approach for fault tolerant control of LPV systems. *Journal of Process Control*, 24:203–222, 2014.

T. Steffen. *Control reconfiguration of dynamical systems: Linear approaches and structural tests*, volume 230 of *Lecture Notes in Control and Information Sciences*. Springer, 2005.

J. F. Sturm. Using SeDuMi 1.02, a MATLAB toolbox for optimization over symmetric cones. *Optimization methods and software*, 11-12:625–653, 1999.

K. Tanaka and H. O. Wang. *Fuzzy control systems design and analysis: A linear matrix inequality approach*. John Wiley and Sons, Inc., 2001. ISBN 0-471-32324-1 (Hardback); 0-471-22459-6 (Electronic).